JOURNAL OF MATERIALS SCIENCE 28 (1993) 3793–3804

Phase structure and morphological variations induced by straining in injection-moulded samples of PA6/EVA blends: influence of molecular structure of EVA copolymers

M.L. ADDONIZIO, L. D'ORAZIO, E. MARTUSCELLI
Istituto di Ricerche su Tecnologia dei polimeri e Reologia del C.N.R., via Toiano, 6, 80072 Arco Felice, Napoli, Italy

The influence of molecular structure and composition of ethylene-co-vinyl acetate (EVA) copolymers, differing in molecular mass and, for a given molecular mass, in vinyl acetate content (wt/wt), on morphological and structural changes undergone by injection-moulded samples of Nylon 6 (PA6)/EVA blends during uniaxial tensile straining at room temperature up to sample rupture and on properties of such materials was studied. Direct correlations between molecular structure and composition of EVA copolymers and the shape and size of domains of dispersed phase and ultimate properties of PA6/EVA materials have been drawn. For the dumb-bell-shaped specimens strained just beyond the yielding point, it was found that the original layered structure was strongly modified by straining. Three layers were, in fact, generated: a skin surface, where no domains of EVA dispersed phase were observed, an outer layer, where the EVA domains were elongated along the draw direction assuming mainly cylindrical shape, and a core where the EVA phase was segregated in ellipsoidal-shaped domains having their major axis oriented along the draw direction. For the samples strained to break it was found that the PA6/EVA fibres showed a single glass transition temperature, whose value is lower than that found for the fibre of plain PA6, but higher than that shown by PA6 phase in the unstrained samples; such a value, moreover, tends to be decreased on increasing the vinyl acetate content along the EVA chain, irrespective of copolymer molecular mass. The calorimetric measurements performed revealed, moreover, a noticeable increase of the observed melting temperature values of EVA phase in PA6/EVA fibres. In the PA6/EVA samples strained to break, only two different layers were seen: an outer skin, free of EVA domains, and a core where the EVA dispersed phase segregated in ellipsoidal-shaped domains. The values of stress at break, σ_B, and of the elongation at break, ε_B, exhibited by PA6/EVA fibres were found to be lower than those shown by the plain PA6. The trends of σ_B and ε_B values against the EVA vinyl acetate content showed, moreover, that σ_B and ε_B values decreased with increasing vinyl acetate content along the copolymer chain.

1. Introduction

The results of an investigation concerning the influence of overall blend composition, different processes and processing conditions on melt rheology, phase morphology and structure and impact properties of blends of Nylon 6 (PA6) and ethylene-co-vinylacetate copolymers (EVA) were reported in previous papers [1, 2]. From such studies aimed at correlating processing, mode and state of dispersion of the minor component and properties in the PA6/EVA system, we concluded that the physical–mechanical response of such incompatible polymer blends is determined mainly by the following interrelated factors: melt-phase viscosity ratio, molecular mass of components and molecular mass distribution, molecular structure of EVA copolymers, and overall blend composition.

In order to study the role of the molecular characteristics of the EVA copolymers, we blended PA6 with several EVA copolymers differing in molecular mass, and for a given molecular mass, in the vinyl acetate content (from 20% (wt/wt) up to 40% (wt/wt)). The results of systematic studies dealing with the influence of molecular structure and composition of EVA copolymers in this type of blend on rheological behaviour in the molten state, on mode and state of dispersion of the EVA minor component developed during extrusion in a double-screw extruder and injection-moulding processes, and on the elastic and tensile yielding behaviour of injection-moulded samples have already been reported [3, 4].

In the present paper we present the results of an investigation undertaken to establish the role that the

0022–2461

molecular mass and/or vinyl acetate (VAc) content along the EVA chain plays in affecting the morphological and structural changes undergone by samples of PA6/EVA blends obtained by injection-moulding technologies during uniaxial tensile straining at room temperature up to rupture. Therefore, the effects of molecular mass and/or VAc content along the EVA chain on the mode and state of dispersion of the minor component, developed both in samples strained at initial cold-drawing and at break, and on thermal behaviour and crystallinity of the fibres, were studied in detail. Finally, an attempt to correlate the molecular parameters of EVA copolymers directly with the ultimate tensile properties of these materials was also accomplished. The definitive goal of the research is to predict, knowing the molecular parameters of the single components, the phase morphology and structure of PA6/EVA blends and then the properties of processed blended material.

2. Experimental procedure

2.1. Materials

The materials used in this study were Nylon 6 (PA6), produced by SNIA, with a number average molecular weight, M_n, of 18 000, and seven different commercial ethylene–vinyl acetate copolymers (EVA) kindly supplied by SNIA.

The codes of the copolymers, the weight percentage of vinyl acetate, the melt-flow index, the observed melting temperature, T'_m, and the glass transition temperature, T_g, are listed in Table I, together with T'_m and T_g values for PA6.

2.2. Blending and sample preparation

The blends, all containing 10 wt% EVA, were obtained by extruding the two components in a double-screw extruder (Creusot-Loire diameter = 56 mm) operating at 83 r.p.m. and at a temperature of 240 °C.

The extrudate materials were injection moulded by means of an injection press (Biraghi) at a temperature of 230 °C with a processing cycle of 30 s in sheets 1 mm thick. The temperature of the mould was 40 °C. From the sheets obtained, dumb-bell-shaped specimens (DIN 53448 T2) for morphological and tensile tests were cut by means of a punch press. Before examining, all the specimens were conditioned in water at 90 °C in order to obtain the same amount of absorbed water (about 3 wt%) according to a procedure described elsewhere [5].

TABLE I Molecular characteristics, glass transition, T_g, and observed melting temperatures, T'_m, of the plain polyamide 6 (PA6) and the ethylene–vinyl acetate copolymers (EVA)

Code	% vinyl acetate (wt/wt)	melt index (g 10 min^{-1})	T_g (°C)	T'_m (°C)
PA6	–	–	42	222
EVA1	20	300–500	−19	80
EVA2	20	3–4	−15	88
EVA3	30	300–500	−19	60
EVA4	30	30–40	−17	60
EVA5	30	3–4	−15	63
EVA6	35	30–40	−16	53
EVA7	40	30–40	−15	55

2.3. Techniques

2.3.1. Calorimetric measurements

The glass transition temperatures, T_g, the observed melting temperatures, T'_m, and the crystallinity index of pure PA6 and its blends with EVA copolymers were obtained by using a differential scanning calorimeter (DSC) Mettler TA 3000.

The thermal analyses were carried out on fibres that had been drawn to break. The following procedure was used: the samples of pure PA6 and PA6/EVA blends (about 15 mg) were heated from −100 °C to 300 °C at a rate of 20 °C min^{-1} and the heat (dH/dt), evolved during the scanning process was recorded as a function of temperature. The T_g was taken as the temperature corresponding to 50% transition. The observed melting temperature, T'_m, and the apparent enthalpies of fusion, ΔH^*, were obtained from the flex point and area of the melting peaks, respectively.

The crystallinity index of PA6 phase (X_c(PA6)) and of overall blend (X_c (blend)) was calculated from

$$X_c(\text{PA6}) = \frac{\Delta H^* (\text{PA6})}{\Delta H^0 (\text{PA6})} \quad (1)$$

$$X_c (\text{blend}) = \frac{\Delta H^* (\text{blend})}{\Delta H^0 (\text{PA6})} \quad (2)$$

where ΔH^* (PA6) is the apparent enthalpy of fusion per gram of PA6 in the blend, ΔH^0 (PA6) is the heat of fusion per gram of 100% crystalline PA6 (from literature data [6] ΔH^0 (PA6) = 188 Jg^{-1}), and ΔH^* (blend) is the apparent enthalpy of fusion per gram of blend.

2.3.2. Mode and state of dispersion of the minor component

The mode and state of dispersion of the minor component were investigated by means of scanning electron microscopy (SEM 501 Philips). The morphological analyses were carried out on surfaces microtomed perpendicular and tangentially to the mould flow direction and on cryogenically fractured surfaces of samples drawn to the following points of the stress–strain curves (see Fig. 1): (a) just after the yielding point, (b) fibre rupture. All the surfaces were examined after coating with gold–palladium.

To elucidate further the mode and state of dispersion of the EVA copolymers in the PA6 matrix, a selective dissolution of the dispersed phase was also carried out according to a method described in a previous paper [1].

2.3.3. Mechanical tensile behaviour

By using an Instron machine (Model 1122), at a constant crosshead speed of 20 mm min^{-1} and room temperature, the stress–strain curves for pure PA6 and PA6 crystallized in the presence of EVA copoly-

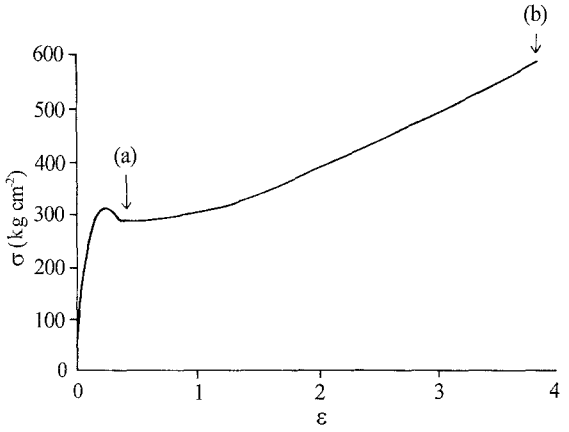

Figure 1 Stress–strain curves for plain PA6.

mers were obtained. From such curves, the Young's modulus, E, the stress at yield, σ_Y, and the elongation at yield, ε_y, (reported in a previous paper [4]), stress, σ_B, and elongation, ε_B, at break were calculated from an average of ten specimens.

3. Results and discussion

3.1. Mode and state of dispersion of the minor component in samples strained just beyond the yielding point

The analysis of the mode and state of EVA dispersion generated in the dumb-bell-shaped injection-moulded samples of PA6-based blends has been reported earlier in a previous paper dealing with morphology and elastic tensile behaviour of such an incompatible polymer system [4]. In all investigated PA6/EVA samples, a layered structure in a direction perpendicular to the mould flow direction according to the schematic model reported in Fig. 2, was developed.

As shown, in Fig. 2, moving from the border toward the core of the samples, four different layers were found.

1. A skin surface, where almost no domains of EVA dispersed phase were observed (layer M in Fig. 2).
2. An outer layer, where the EVA dispersed phase segregated in ellipsoidal and/or cylindrical-shaped domains (layer S in Fig. 2) oriented with their major axes in the direction of the mould flow direction according to the mould flow pattern proposed by Tadmor [7]. It will be recalled that in such a layer the mode and state of dispersion of the minor component depends on both EVA molecular mass and VAc content along the copolymer chain [4].
3. An intermediate transition layer, where the ellipsoidal and/or cylindrical-shaped domains tend to assume a more or less spherical shape (layer I in Fig. 2).
4. A core showing EVA droplet-like morphology (layer C in the Fig. 2), the particle size being mainly determined by copolymer molecular mass, irrespective of VAc content.

The analysis by SEM of the mode and state of EVA dispersion developed in samples strained just beyond the yield point (see Fig. 1), performed on smoothed and subsequently etched transverse and longitudinal surfaces shows that the original layered structure becomes modified according to the schematic model reported in Fig. 3. As shown in Fig. 3, moving from the border towards the core of samples three layers are found instead of four.

1. A skin surface, where no domains of EVA dispersed phase are observed (M).
2. An outer layer, where the EVA domains are elongated along the draw direction assuming mainly cylindrical shape (S).
3. A core where the EVA phase segregated in ellipsoidal-shaped domains (C).

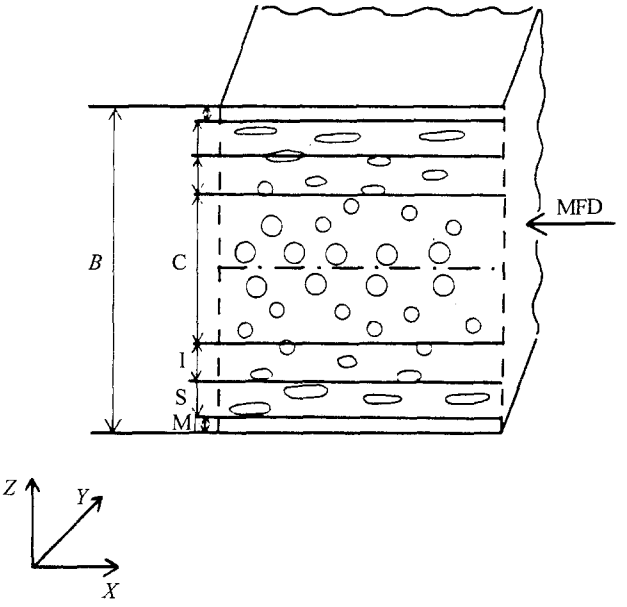

Figure 2 A schematic model of the layered structure shown by all examined samples of PA6/EVA blends in a direction perpendicular to the melt flow direction. B, thickness of the sheet (1 mm); I, intermediate transition layer; S, outer layer; C, core; M, skin surface (pure PA6); MFD, mould flow direction.

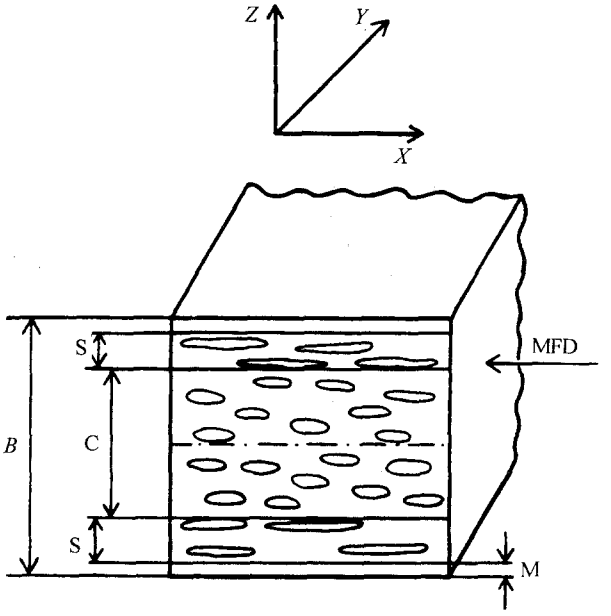

Figure 3 A schematic model of the layered structure shown by all examined samples strained to cold-drawing of PA6/EVA blends in a direction perpendicular to the melt flow direction. $B = 0.8$ mm. Key as for Fig. 2.

The finding that at the outer skin of the sample no domains of the dispersed phase were observable is in agreement with the results reported in the previous papers dealing with PA6/EVA injection-moulded samples [2, 4]. The thickness of such a layer (M), that appears free of EVA domains, is reported in Tables II–IV for all examined blends. As shown, this thickness is about 1 μm for all examined samples; only the EVA4-containing blend exhibited a comparatively thicker M layer (2.0 μm). Such a finding is in agreement with that obtained for the unstrained samples, thus indicating that there is no effect of straining up to cold-drawing on the thickness of such a layer.

3.1.1. Effect of the EVA VAc content

From the analysis of the thickness of the layer S (see Fig. 3), and of the extent of the deformation undergone in such a layer by the domains of EVA copolymers having almost the same melt viscosity the following results can be seen.

TABLE II Layered distribution in injection-moulded samples of PA6/EVA blends with reference to Fig. 3. Layer code, layer thickness, shape and size of the EVA domains for PA6/EVA1 and PA6/EVA3 blends. The samples were strained up to the cold-drawing region (point (a) on the curve of Fig. 1)

Layer code	Layer thickness (%) (half sample)	Shape of EVA domains	Size of EVA domains (μm)
M	PA6/EVA1 1.0	–	–
	PA6/EVA3 1.0	–	–
S	PA6/EVA1 10	Fibre	Breadth 0.4–1.0 Length 0.6–18
	PA6/EVA3 14	Fibre	Breadth 0.2–0.8 Length 8–20
C	PA6/EVA1 39	Ellipsoidal	Minor axis 1.2–2.4 Major axis 1.6–6.4
	PA6/EVA3 35	Ellipsoidal	Minor axis 0.8–1.8 Major axis 1.6–8.8

TABLE III Layered distribution in injection-moulded samples of PA6/EVA blends with reference to Fig. 3. Layer code, layer thickness, shape and size of the EVA domains for PA6/EVA4, PA6/EVA6 and PA6/EVA7 blends. The samples were strained up to the cold-drawing region (point (a) on the curve of Fig. 1)

Layer code	Layer thickness (%) (half sample)	Shape of EVA domains	Size of EVA domains (μm)
M	PA6/EVA4 2.0	–	–
	PA6/EVA6 1.3	–	–
	PA6/EVA7 1.3	–	–
S	PA6/EVA4 10	Ellipsoidal	Minor axis 0.4–0.8 Major axis 0.8–2.4
	PA6/EVA6 11.7	Ellipsoidal	Minor axis 0.2–0.6 Major axis 0.8–2.0
	PA6/EVA7 11.7	Fibre	Breadth 0.2–0.6 Length 4.0–16
C	PA6/EVA4 38	Ellipsoidal	Minor axis 0.4–1.6 Major axis 1.6–5.0
	PA6/EVA6 37	Ellipsoidal	Minor axis 0.4–1.2 Major axis 1.2–5.0
	PA6/EVA7 37	Ellipsoidal	Minor axis 0.4–1.6 Major axis 1.2–4.4

TABLE IV Layered distribution in injection-moulded samples of PA6/EVA blends with reference to Fig. 3. Layer code, layer thickness, shape and size of the EVA domains for PA6/EVA2 and PA6/EVA5 blends. The samples were strained up to the cold-drawing region (point (a) on the curve of Fig. 1)

Layer code	Layer thickness (%) (half sample)	Shape of EVA domains	Size of EVA domains (μm)
M	PA6/EVA2 1.0	–	–
	PA6/EVA5 1.0	–	–
S	PA6/EVA2 15	Fibre	Breadth 0.4–0.8 Length 8–20
	PA6/EVA3 8	Fibre	Breadth 0.6–1.0 Length 8–14
C	PA6/EVA2 34	Ellipsoidal	Minor axis 1.2–1.8 Major axis 4–10
	PA6/EVA5 41	Ellipsoidal	Minor axis 0.6–2.4 Major axis 2–8

(i) In the case of the blends containing copolymers having comparatively lower melt viscosity (EVA1 and EVA3), slightly higher thickness is shown by the EVA 3-containing blend (see Table II). Moreover, such a thickness is about twice as high as that respectively shown by unstrained samples. Note that both EVA1- and EVA3- dispersed phases form fibres having quite comparable breadth, but different length. In fact, the length range shown by EVA3 copolymers is considerably narrower than that exhibited by EVA1 copolymer (see Table II); moreover fibres with higher average length are developed in a sample containing EVA3 phase. Taking into account that the unstrained samples of the PA6/EVA1 and PA6/EVA3 blends showed different states of dispersion of the minor component as the EVA1 and EVA3 phases segregated, respectively, in cylindrical and ellipsoidal-shaped domains [4], the above finding indicates that the straining to cold-drawing results for EVA1-dispersed phase in a slight thinning of the EVA1 rods, whereas the EVA3 ellipsoidal-shaped domains are considerably elongated along the draw direction giving rise to fibres. Thus, contrary to what is observed for the unstrained samples [4], higher deformation occurs in the EVA phase having the higher VAc content along its chain (EVA3).

(ii) Among the blends containing copolymers with intermediate melt viscosity (EVA4, EVA6 and EVA7) (see Table III), the blend containing EVA4 shows a thickness of the S layer slightly lower than that shown by blends containing EVA6 and EVA7. It should be recalled that no change caused by straining up cold-drawing in the S thickness is observed for PA6/EVA4 blends, whereas such thickness increases in blends containing EVA6 and EVA7, the highest S increase being shown by the EVA6-containing blend [4]. It should be noted that EVA4- and EVA6-dispersed phases segregate in ellipsoidal- shaped domains with comparable ranges of the minor and major axis (see Table III), whereas EVA7 copolymers in the draw direction form fibres having a narrow breadth range (0.2–0.6 μm) and wide length range (4–16 μm) (see Table III). Such morphological results indicate that EVA4 and EVA6 phases offer a resistance to deforma-

tion higher than that shown by EVA7 phase. Thus, as was previously observed in the case of the PA6-based blends containing the copolymer having a comparatively lower molecular mass, higher deformation is found to be associated with higher VAc content along the copolymer chain (EVA7). Such a hypothesis could also be supported by the finding that, in the unstrained samples, EVA4 and EVA7 were segregated in ellipsoidal-shaped domains, whereas EVA6 showed a droplet-like morphology [4].

(iii) For the blends containing the copolymer with comparatively higher melt viscosity (EVA2 and EVA5), a thicker S layer is shown by the blend containing EVA2 (see Table IV). It should be noted that by straining to cold-drawing the samples of PA6/EVA2 and PA6/EVA5 blends, the thickness becomes, respectively, 2.5 and 4.0 times as high as that shown by the unstrained samples [4]. Both EVA2 and EVA5 phases form fibres having comparable breadth, but different length ranges, resulting in a comparatively wider length range shown by EVA2 phase (see Table IV). Such a finding, indicates that the EVA5 phase offers a higher resistance to deformation. Thus, in agreement with the morphological results obtained for the same unstrained samples, an increase of the VAc content along the EVA chain from 20% up to 30% (wt/wt), may be associated with an increased copolymer elasticity, irrespective of the deformation undergone.

From all the above results, the following general trend can be drawn: in the S layer (see Fig. 3), the extent of deformation undergone by domains of EVA-dispersed phase increases with increasing VAc content along the EVA chains for samples containing copolymer with comparatively lower and intermediate molecular mass, whereas for samples containing copolymer with higher molecular mass, such a deformation decreases on increasing the VAc content in EVA.

Moving further on up to core of the dumb-bell-shaped specimens, the EVA-dispersed phase segregates mainly in ellipsoidal-shaped domains. The ranges of the minor and major axes of the ellipsoids for all investigated samples are reported in Tables II–IV. From these data, the following points can be seen.

(i) In the case of blends containing EVA copolymers having comparatively lower melt viscosity (EVA1 and EVA3), higher deformation is undergone by the sample with a copolymer having a higher VAc content along its chain (EVA3); narrower and wider ranges of minor and major axes being observed, respectively (see Table II).

(ii) For the blends containing copolymers of intermediate molecular mass (EVA4, EVA6 and EVA7), the resulting ranges of the minor and major axes of the EVA ellipsoidal-shaped domains are comparable, indicating that the mode of dispersion of the minor component is independent of the VAc content along the EVA chain (see Table III).

(iii) For the blends containing copolymers of comparatively higher molecular mass (EVA2 and EVA5), the ellipsoidal-shaped domains formed by EVA2 and EVA5 copolymers have a quite comparable average minor axis, a higher average major axis being shown by the sample with EVA2 phase (see Table IV). Such a finding indicates that for such samples the deformation caused by straining to cold-drawing tends to be decreased with increasing VAc content along the EVA chain.

Thus the deformation undergone along the draw direction by domains of dispersed phase in the core for blends containing EVA of low and high molecular mass, increases and decreases, respectively, with increasing VAc content along the EVA chain, whereas for the blends containing the copolymer with intermediate molecular mass, such a deformation seems to be almost independent of EVA VAc content.

3.1.2. Effect of the EVA molecular mass

Looking at the influence of the EVA molecular mass on the mode and state of dispersion and on the deformation undergone by the domains of the EVA minor component in the S layer (see Fig. 3), two points can be observed

(i) For a VAc content of 20% (wt/wt) (EVA1 and EVA2), the thickness of the S layer increases with increasing copolymer molecular mass. Moreover, the breadth of the fibres formed by EVA1- and EVA2-dispersed phases are quite comparable, whereas the length range shown by EVA2 is narrower than that exhibited by EVA1 (see Tables II and IV).

Taking into account that, in the unstrained samples, EVA1 and EVA2 showed different state of dispersion, the EVA1 and EVA2 copolymers segregating, respectively, in cylindrical and ellipsoidal-shaped domains [4], the above morphological results indicate that the EVA copolymer with lower molecular mass offers a higher resistance to deformation induced by straining to cold-drawing. It should be recalled that in the unstrained samples, a higher resistance to deformation was shown by the sample containing the copolymer with higher molecular mass.

(ii) For an EVA with a VAc content of 30% (wt/wt), the thickness of the S layer decreases with increasing copolymer molecular mass. It should be noted that the EVA with comparatively lower and higher molecular mass forms fibres showing comparable ranges of breadth but different length ranges, longer fibres being developed in the blend containing the EVA with the lower molecular mass (EVA3). On the other hand, ellipsoidal-shaped domains are shown by the blend containing the copolymer with intermediate molecular mass (see Tables II–IV). Such a finding indicates that higher deformation is undergone by the domains of the EVA copolymer of lower molecular mass, in agreement with the results obtained for unstrained samples.

From the above, one can infer that, for a given VAc content along the EVA chain, the deformation undergone in the S layer according to Fig. 3 depends on the copolymer molecular mass. It should be pointed out that, for lower VAc content (20% wt/wt), such a deformation tends to increase with increasing EVA

molecular mass, whereas for higher VAc content (30% wt/wt) it tends, on the contrary, to decrease with increasing EVA molecular mass.

Looking at the influence of EVA molecular mass on the mode and state of dispersion of the minor component developed in the core of the sample with reference to Fig. 3, it can be observed that, for lower VAc content along EVA chain (20% (wt/wt)), the straining to cold-drawing induces higher deformation of domains of dispersed phase with a higher molecular mass (see Tables II and IV). With increasing the VAc content along the EVA chain (30% (wt/wt)), no systematic dependence of the deformation caused by straining up to cold-drawing on EVA molecular mass can be observed. In fact, a quite comparable deformation is undergone by the EVA domains with lower and higher melt viscosity, the highest resistance to deformation being shown by the EVA phase of intermediate molecular mass (compare the range of the ellipsoid minor and major axes shown by the EVA6 phase with those shown by EVA3 and EVA5 phases in Tables II–IV). It should be recalled that the core of all the unstrained samples showed a droplet-like morphology (see Fig. 2), the particle size being determined by EVA molecular mass, irrespective of VAc content along the copolymer chain [4].

3.2. Thermal behaviour and crystallinity of samples strained to break

Typical DSC thermograms of the dumb-bell-shaped specimens of plain PA6 and PA6/EVA blends strained to break are shown in Fig. 4. As shown, the PA6 fibre exhibits a glass transition temperature, T_g, of 57°C and from the DSC thermograms of the PA6/EVA fibres, a single T_g can be detected. The values of T_g, to be attributed to the PA6 phase, are reported in Table V where, for sake of comparison, the T_g values for the unstrained samples are also listed.

It should be underlined that, as reported in Table V, from the DSC thermograms of PA6/EVA unstrained samples, two distinct T_g values were clearly shown (see Fig. 5); these T_g values were located in the ranges −11 to −9 °C and 42–45 °C and were attributed to EVA copolymer and PA6 phase, respectively. It should be recalled, moreover, that the T_g value of the EVA components in the unstrained samples occurred about 10°C higher than that shown by the EVA single phase (compare Table V with Table I). Such a finding, taking into account that the T_g shown by the PA6 phase in the unstrained PA6/EVA samples was comparable with that shown by the plain unstrained PA6 (see Table V), suggested that a dissolution of the PA6 molecules with lower molecular mass into the EVA phase could have occurred.

TABLE V Glass transition, T_g, of the plain polyamide 6 (PA6) and PA6/EVA blends for samples strained to rupture and for unstrained samples

Code	Strained, T_g (°C)[a]	Unstrained	
		T_g* (°C)[b]	T_g (°C)[a]
PA6	57		42
PA6/EVA1	50	−9	44
PA6/EVA2	50	−9	45
PA6/EVA3	50	−9	45
PA6/EVA4	49	−10	42
PA6/EVA5	49	−9	45
PA6/EVA6	46	−11	44
PA6/EVA7	47	−9	44

[a] Glass transition temperatures of plain PA6 in the blends.
[b] Glass transition temperature of EVA in the blends.

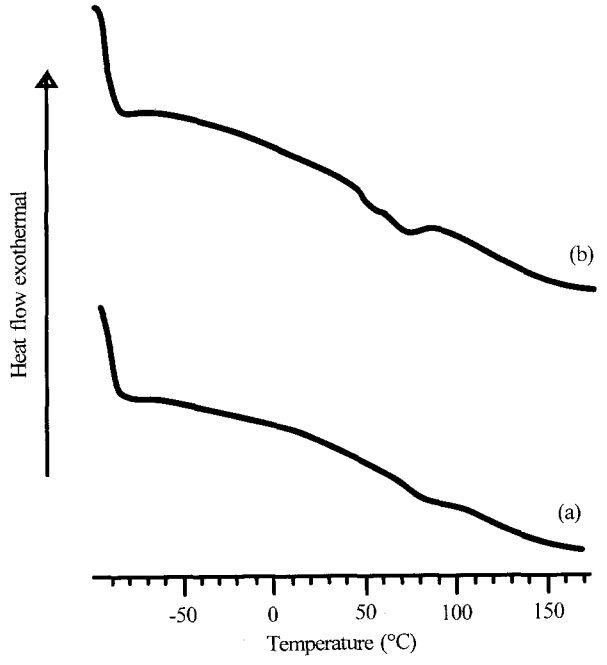

Figure 4 Typical DSC thermograms of fibres of (a) PA6 and (b) PA6/EVA blends.

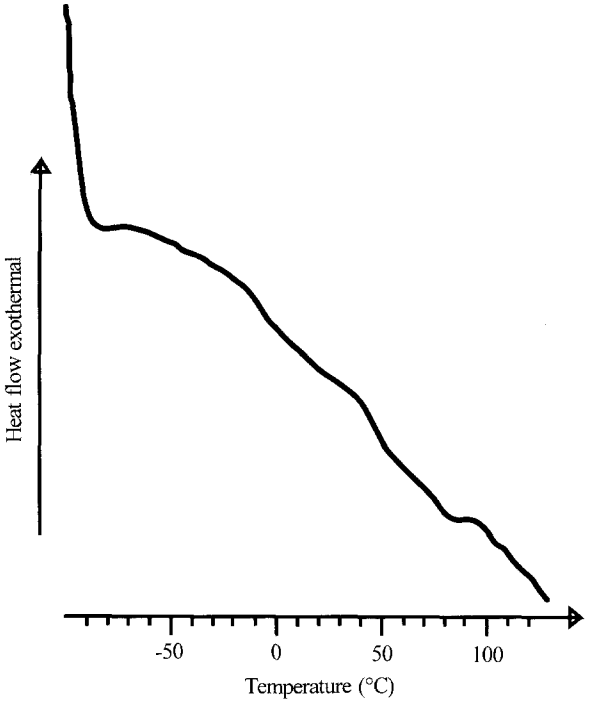

Figure 5 Typical DSC thermograms of PA6/EVA unstrained samples.

By comparing the T_g values of 42 °C, shown by the plain unstrained PA6, with the T_g value shown by the fibre of the plain PA6, the PA6 T_g is shifted to higher temperature by about 15°C (see Tables I and V). Assuming that the morphological and structural changes undergone by the PA6, during deformation to break, follow the molecular model proposed by Shultz for semicrystalline polymers [8], the shift observed in T_g value of the PA6 fibre indicates that, even though the amorphous material provides the major resistance to deformation during all the state changes, it suffers by straining a reduction in its molecular mobility.

On the other hand, the PA6/EVA fibres exhibit T_g values lower than those found for the fibre of plain PA6, but higher than that shown by PA6 phase in the unstrained samples; such values, furthermore, tend to be decreased with increasing VAc content along the EVA chain, irrespective of copolymer molecular mass.

Taking into account that the T_g of the plain PA6 is increased by straining, the finding that in PA6/EVA fibres the PA6 T_g decreases and that such a decrease becomes larger with increasing VAc content along the EVA chain, can be accounted for by supposing that EVA molecules having higher VAc content along their chain are dissolved into the amorphous phase of the PA6.

The finding that, as shown in Fig. 4, from the DSC thermograms of PA6/EVA fibres, no T_g can be detected to be attributable to EVA phase, seeming to suggest that a dissolution of PA6 molecules having low molecular mass into the EVA also occurs. Owing to such a dissolution, it seems reasonable to suppose that the EVA T_g is further shifted to higher temperature becoming no longer detectable.

The calorimetric measurements revealed, moreover, that the PA6 fibres show a single sharp fusion peak, whereas the fibres of PA6 crystallized in the presence of EVA phase show double fusion peaks broader than that exhibited by the plain PA6 fibre. It should be recalled that both the unstrained PA6 and PA6/EVA samples showed multiple fusion peaks [4]. Such results indicate that in the course of heating no recrystallization phenomenon and/or polymorphic transition in the PA6 fibre occurs, whereas such phenomena are still present with a reduced intensity in PA6/EVA fibres. The temperature position of the endotherm peak shown by plain PA6 and the highest temperature position shown by PA6/EVA samples are characteristic of the melting of the more stable α crystalline form of the PA6. Such values are compared to that shown by α crystals of unstrained PA6 and PA6/EVA samples in Table VI. As shown in this table, the T'_m values shown by all the unstrained and strained samples are quite comparable, indicating that the perfection and thickness of crystals of both plain PA6 and PA6 crystallized in the presence of EVA copolymers are unaffected by straining.

Endothermic peaks, due to the melting of ethylene blocks of EVA copolymers in PA6/EVA thermograms, are also observable; the corresponding temperature positions are reported in Table VI, where for sake of comparison, the T'_m values shown by the EVA phase in the unstrained samples are also reported. As seen in this table, such T'_m values are unaffected by straining. It should again be noted that by comparing the T'_m values exhibited by the neat EVA copolymers with the T'_m values exhibited by the EVA phase in the unstrained and strained blends (see Tables I and VI) it emerges that on increasing the VAc along the copolymer chain from 20% (wt/wt) to 40% (wt/wt) the T'_m values strongly increase. Moreover, for a VAc content of 30% (wt/wt), such an increase depends on the copolymer molecular mass, higher T'_m being shown by EVA copolymer having comparatively lower molecular mass. Such a surprisingly noticeable increase of T'_m values shown by EVA phase in PA6/EVA fibres also supports the view that, in agreement with the T_g values of the PA6/EVA fibres previously discussed, EVA molecules with a higher number of VAc groups along their chain are dissolved into the amorphous PA6, leaving copolymers with longer PE sequences along their chain.

The finding that the EVA3 shows a comparatively higher T'_m value could be explained by supposing that there is probably a higher concentration of VAc groups in the chains with lower molecular mass.

The X_c values shown by the fibres of plain PA6 and PA6/EVA blends are compared with that shown by the unstrained samples in Table VII. Note that the

TABLE VI Observed melting temperatures, T'_m, of the plain polyamide 6 (PA6) and PA6/EVA blends for strained and unstrained samples

Code	Strained		Unstrained	
	T'_m (°C) [a]	T'_m (°C) [b]	T'_m (°C) [a]	T'_m (°C) [b]
PA6		223		222
PA6/EVA1	78	223	80	225
PA6/EVA2	91	221	90	222
PA6/EVA3	87	222	85	224
PA6/EVA4	75	222	75	223
PA6/EVA5	80	221	80	222
PA6/EVA6	70	225	70	222
PA6/EVA7	78	222	80	222

[a] Observed melting temperatures of EVA in the blends.
[b] Observed melting temperatures of PA6 in the blends.

TABLE VII Crystallinity index of plain PA6 phase (X_c (PA6)) and PA6/EVA blends X_c (blend) of the plain PA6 and PA6 crystallized from its blends with EVA copolymers for strained and unstrained samples

Code	Strained		Unstrained	
	X_c (blend) (%)	X_c (PA6) (%)	X_c (blend) (%)	X_c (PA6) (%)
PA6		40		45
PA6/EVA1	40	45	38	42
PA6/EVA2	44	49	40	44
PA6/EVA3	38	42	34	37
PA6/EVA4	34	38	36	40
PA6/EVA5	40	45	37	41
PA6/EVA6	42	47	40	44
PA6/EVA7	35	39	37	42

crystallinity of plain PA6 is reduced on straining about 5%. Such a decrease may be explained supposing that the conformationally ordered and extended chains of PA6, pulled out by lamellar shearing, lose their lateral order and thus become amorphous.

As is also shown in Table VII, for a given VAc content along the EVA chain, no regular dependence of X_c (blend) values on the EVA molecular mass can be found. On the other hand, for a given molecular mass, there is a systematic dependence of X_c (blend) values only for the blends containing EVA with comparatively higher and lower molecular mass. For these samples, in fact, the X_c values are found to decrease with increasing VAc content along EVA chain.

The X_c values shown by PA6 phase in PA6/EVA fibres, except for PA6/EVA6 and PA6/EVA7 samples, are higher than that of plain PA6. In the case of the blends containing copolymers with comparatively higher and lower molecular mass, such values, as expected, depend on VAc content along the EVA chain, higher X_c (PA6) values being shown by the sample containing EVA with lower VAc content.

Taking into account that the crystallinity of plain PA6 is reduced by straining to break from 45% to 40%, and that the X_c (PA6) values of the unstrained samples were lower than that of plain PA6 (see Table VII), the above findings could be explained by assuming that under stress in the presence of EVA phase, some PA6 chains are able to recrystallize and/or new PA6 ordered phase can be formed during deformation. Such a hypothesis seems to be supported also by the shape and broadness of the melting peaks of the PA6/EVA fibres.

3.3. Mode and state of dispersion of the minor component in samples strained to break

By further straining the dumb-bell-shaped specimens to break, the layered structure developed in the samples strained to cold-drawing results, becomes modified according to the model schematically shown in Fig. 6. As seen, only two layers are found: (1) an outer skin free of EVA domains whose thickness remains unaffected by strain (compare Tables II–IV with Table VIII); and (2) a core where the EVA-dispersed phase segregates in ellipsoidal-shaped domains. Such a finding indicates that the straining of the samples to rupture results in the break-up and relaxation of the EVA cylindrical-shaped domains generated in the samples strained to cold-drawing in the S layer.

3.3.1. Effect of the EVA VAc content

In the core of the blends containing the copolymers having comparatively lower melt viscosity (EVA1 and EVA3) it can be seen that both the average minor and major axis shown by EVA3 ellipsoidal-shaped domains are larger than those shown by EVA1 domains. This indicates that the dispersion coarseness and deformation undergone by the dispersed phase tend to increase with increasing VAc content along the EVA chain (see Table VIII). Note, moreover, that by straining to rupture, the ellipsoidal-shaped domains, shown

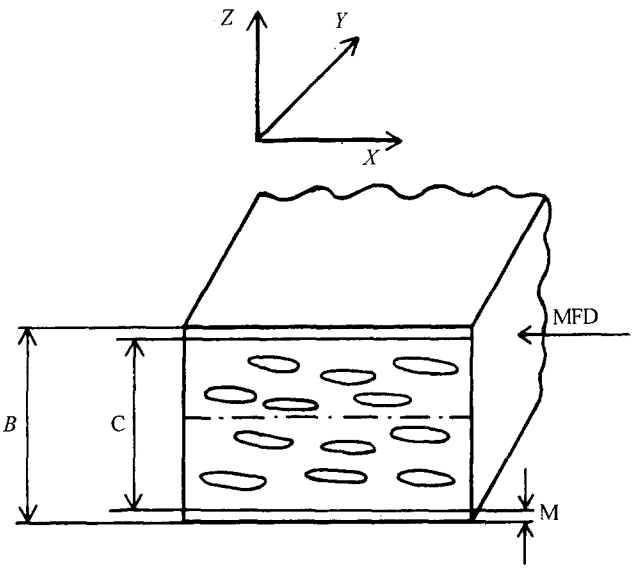

Figure 6 A schematic model of the layered structure shown by all examined samples strained to break of PA6/EVA blends in a direction perpendicular to the mould flow direction. $B = 0.6$ mm. Key as for Fig. 2.

TABLE VIII Layered distribution in injection-moulded samples of PA6/EVA blends with reference to Fig. 6. Layer code, layer thickness, shape and size of the EVA domains for PA6/EVA1, PA6/EVA3, PA6/EVA4, PA6/EVA6, PA6/EVA7, PA6/EVA2 and PA6/EVA5 blends.

Layer code	Layer thickness (%) (half sample)	Shape of EVA domains	Size of EVA domains (μm)
M	PA6/EVA1 1.0	–	–
	PA6/EVA3 1.0	–	–
	PA6/EVA4 2.0	–	–
	PA6/EVA6 1.0	–	–
	PA6/EVA7 1.0	–	–
	PA6/EVA2 1.0	–	–
	PA6/EVA5 1.0	–	–
C	PA6/EVA1 49	Ellipsoidal	Minor axis 0.6–1.2
			Major axis 3.0–8.0
	PA6/EVA3 49	Ellipsoidal	Minor axis 0.6–2.6
			Major axis 2.0–11
	PA6/EVA4 48	Ellipsoidal	Minor axis 0.6–1.4
			Major axis 1.6–6.0
	PA6/EVA6 49	Ellipsoidal	Minor axis 0.6–1.2
			Major axis 1.6–3.4
	PA6/EVA7 49	Ellipsoidal	Minor axis 0.6–1.2
			Major axis 2.0–5.0
	PA6/EVA2 49	Ellipsoidal	Minor axis 0.6–2.0
			Major axis 3.0–3.9
	PA6/EVA5 49	Ellipsoidal	Minor axis 0.6–2.0
			Major axis 2.6–8.0

in the core of the samples strained to cold-drawing, are elongated further along the draw direction. In fact, narrower and wider ranges of minor and major axes of such domains can be observed, respectively (compare Table VIII with Table II).

For the blends containing EVA copolymer with intermediate melt viscosity (EVA4, EVA6 and EVA7), the ellipsoidal-shaped domains of the dispersed phase show comparable ranges of minor axis, whereas the major axis of such domains has comparable size only in the samples containing EVA4 and EVA7 copolymers, lower deformation being undergone by the domains of the samples of the PA6/EVA6 blend (see

Table VIII). These findings indicate that there is no systematic dependence of the dispersion coarseness and of the deformation undergone by the minor component, on the VAc content along the copolymer chain. It must be stressed, moreover, that no further deformation of the ellipsoidal-shaped domains developed in the core of the samples strained to cold-drawing is induced by straining to break (compare Tables III and VIII).

Quite comparable dispersion coarseness and deformation of the minor component is shown by the blends containing the copolymers having a higher melt viscosity (see the range of the minor and major axes, respectively, exhibited by PA6/EVA2 and PA6/EVA5 samples in Table VIII). This indicates that the mode and state of dispersion of EVA2 and EVA5 copolymer are independent of VAc content along the EVA chain. Note, furthermore, that as already observed for the blends containing the copolymers with intermediate molecular mass (EVA4, EVA6 and EVA7), no change in the mode and state of dispersion of the minor component, observed in the core of the samples strained to cold-drawing, is caused by further straining to break (compare Tables IV and VIII).

From the above, one can infer that the dispersion coarseness and deformation undergone by domains of dispersed phase are determined by the VAc content along the EVA chain only in samples containing the copolymer with comparatively lower molecular mass.

3.3.2. Effect of the EVA molecular mass

Looking at the influence of EVA molecular mass on the mode and state of dispersion of the minor component and on deformation undergone, it can be seen that for a vinyl acetate content of 20% (wt/wt) along the copolymer chain (EVA1 and EVA2), almost comparable ranges of minor and major axes of the ellipsoidal-shaped domains are observed (see Table VIII). In the case of PA6/EVA blends containing copolymers with 30% (wt/wt) VAc along their chain (PA6/EVA3, PA6/EVA4 and PA6/EVA5), no systematic dependence of the mode and state of dispersion of the minor component can be observed. In fact, finer dispersion and lower deformation are shown by the sample containing the EVA phase of intermediate molecular mass (see Table VIII). All the above results indicate that in the core of the samples strained to break, irrespective of the VAc content along the copolymer chain, finer dispersion is shown by the blend containing EVA copolymer of intermediate molecular mass. Such a result agrees with that already obtained while studying injection-moulded samples of both the same and different PA6/EVA blends [3, 4].

3.4. Ultimate tensile mechanical properties

Stress–strain curves for plain PA6 and PA6 crystallized in the presence of EVA copolymers are shown by Figs 7–9. The values of the elastic modulus, E, the stress at yield, σ_y, and elongation at yield, ε_y, for plain PA6 and PA6/EVA blends have been discussed in the previous paper [4].

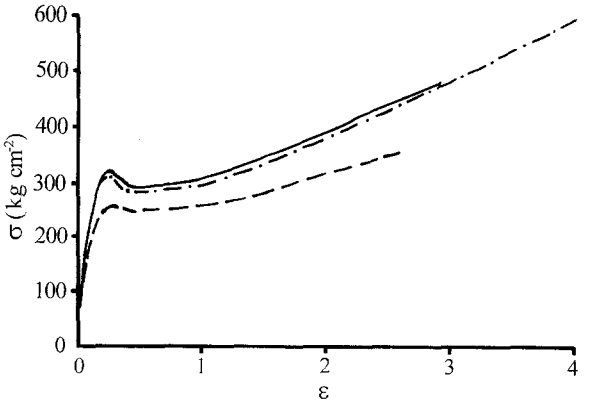

Figure 7 Stress–strain curves for plain PA6 and PA6/EVA blends: (—●—) PA6, (——) PA6/EVA3, (– – –) PA6/EVA1.

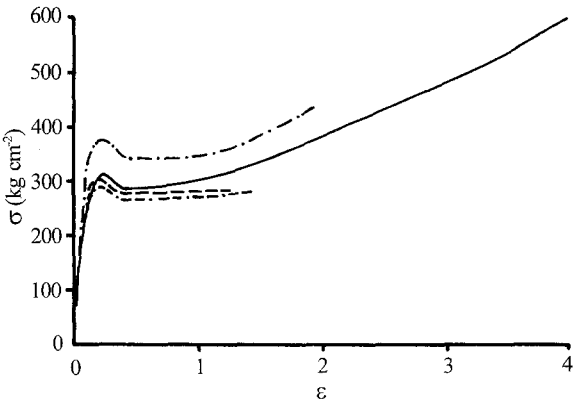

Figure 8 Stress–strain curves for plain PA6 and PA6/EVA blends: (——) PA6, (—●—) PA6/EVA4, (– – –) PA6/EVA7, (---●---) PA6/EVA6.

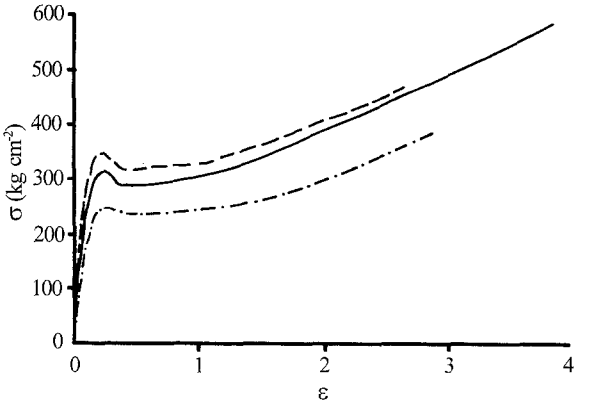

Figure 9 Stress–strain curves for plain PA6 and PA6/EVA blends: (——) PA6, (– – –) PA6/EVA5, (—●—) PA6/EVA2.

As shown by Figs 7–9, both plain PA6 and PA6 crystallized from its blends with EVA copolymers exhibit, after the yielding point, a cold-drawing region and fibre rupture. Moreover, as expected for semi-crystalline polymers, the cold-drawing phenomenon is preceded by formation of necking (see Fig. 10).

The plain PA6 sample shows no stress whitening, at either cold-drawing or fibre rupture, whereas all PA6/EVA samples show at cold-drawing in their central part a more or less stress-whitened zone, the fibres becoming completely stress-whitened at break. The

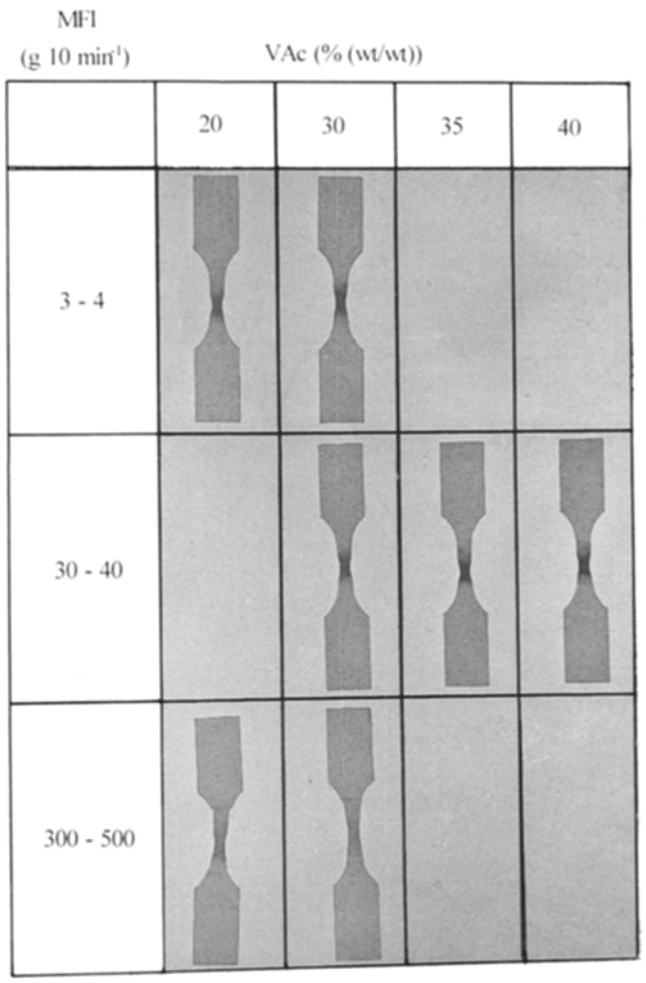

Figure 10 Transparency photograph of dumb-bell-shaped specimens of PA6/EVA blends at the cold-drawing point, together with the MFI and VAc content of the EVA copolymers.

stress-whitening phenomenon is associated with multicraze formation and/or cavitation during the tensile tests. It must be noted that, at cold-drawing, the intensity of such a phenomenon increases with decreasing coarseness of the EVA domains and deformation along the draw direction (see Fig. 10 and Tables II–IV).

Such findings, in agreement with that obtained when studying yielding behaviour of PA6/EVA materials [4], confirm that the capability of domains of dispersed phase to initiate multicraze formation and/or be mechanically equivalent to a void, taking into account the very weak adhesion at the interface [2], decreases with increasing dispersion coarseness of minor component and undergoes deformation. The values of the stress at break, σ_B, and elongation at break, ε_B, of the plain PA6 and PA6/EVA blends are reported in Table IX. Note that for all the PA6/EVA samples investigated, the σ_B values are lower than that shown by the plain PA6; moreover such values will be determined by the dispersion coarseness of the EVA minor component. The trend of the σ_B values versus the number average of the major axis of the ellipsoidal-shaped EVA domains, $\bar{D}$, shows, in fact, that the σ_B increases with increasing $\bar{D}$ (see Fig. 11). This indicates that the smaller the EVA domains are in size, the higher are the stress concentrations induced by external load with subsequent lower overall stress.

As shown in Table IX the values of the elongation at break, ε_B, shown by all the PA6/EVA samples investigated are lower than that of plain PA6, indicating that the presence of EVA domains reduces the capability of the material to be plastically deformed. It should be pointed out also that such values are determined by the dispersion coarseness of the EVA copolymers. The trend of the ε_B values against $\bar{D}$ of EVA domains shows, in fact, that ε_B increases with increasing $\bar{D}$ (see Fig. 12), indicating that the hindrance generated by the EVA domains to matrix cold-drawing and then the instability in the flow, which causes premature rupture of the blended material, decreases with increasing major axis of the ellipsoidal-shaped EVA domains.

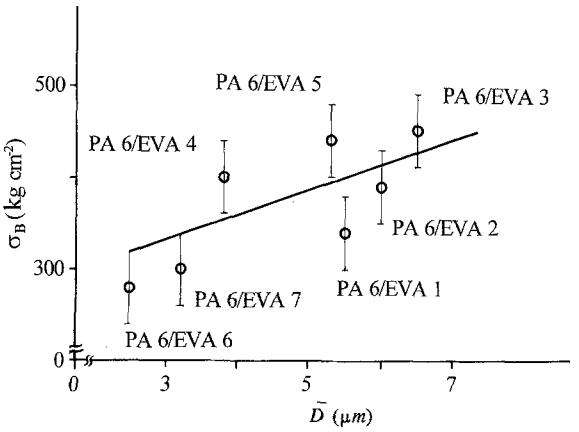

Figure 11 Stress at break of PA6/EVA samples versus the number average of the major axis of EVA domains.

TABLE IX Stress, σ_B, at break, elongation, ε_B, at break and molecular characteristics of pure PA6 and PA6/EVA blends

Code	σ_B 10^2 kg cm^{-2}	ε_B	EVA melt index (g 10 min^{-1})	% vinyl acetate (wt/wt)
PA6	5.8 ± 0.6	3.8 ± 0.4	–	–
PA6/EVA1	3.4 ± 0.4	2.4 ± 0.4	300–500	20
PA6/EVA2	3.9 ± 0.4	3.1 ± 0.3	4–4	20
PA6/EVA3	4.5 ± 0.3	2.9 ± 0.4	300–500	30
PA6/EVA4	4.0 ± 0.8	1.8 ± 0.7	30–40	30
PA6/EVA5	4.4 ± 0.6	2.4 ± 0.4	3–4	30
PA6/EVA6	2.8 ± 0.1	1.0 ± 0.4	30–40	35
PA6/EVA7	3.0 ± 0.4	1.3 ± 0.6	30–40	40

3.4.1. Effect of the EVA VAc content

At cold-drawing, no regular dependence of the intensity of the stress-whitening phenomenon, for a given EVA molecular mass, on VAc content along the EVA chain can be observed. As shown by Fig. 10, for samples with EVA of comparatively higher and intermediate molecular mass, such an intensity increases with increasing VAc content along the EVA chain, whereas an opposite trend is shown by the intensity of stress-whitening phenomenon for blended material containing EVA components of lower molecular mass. Recalling that both σ_B and ε_B values were found to be determined by the EVA dispersion coarseness, and that such a dispersion coarseness in the samples strained to break is mainly determined by the VAc content along the copolymer chain, the VAc content along the EVA chain is seen to be the main molecular parameter affecting both σ_B and ε_B values of the blended material. The trends of σ_B and ε_B with the EVA VAc content show, in fact, that σ_B and δ_B values tend to decrease with increasing VAc content (see Figs 13 and 14).

3.4.2. Effect of the EVA molecular mass

At cold-drawing, the intensity of the stress-whitening phenomenon, for a given VAc content along the EVA chain, tends to increase with increasing EVA molecular mass (see Fig. 10).

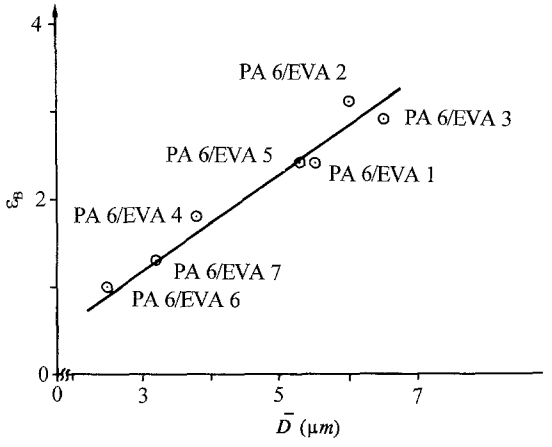

Figure 12 Strain at break of PA6/EVA samples versus the number average of the major axis of EVA domains.

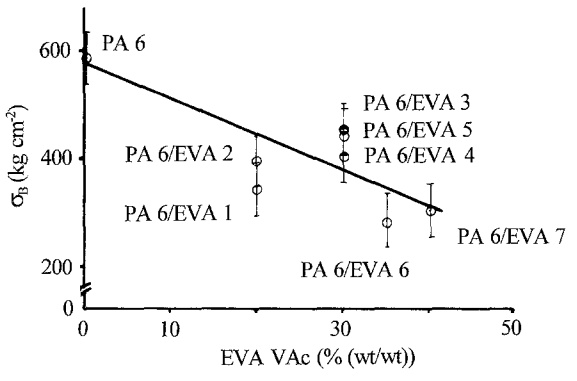

Figure 13 Stress at break versus VAc content of EVA copolymer for the plain PA6 and PA6/EVA blends.

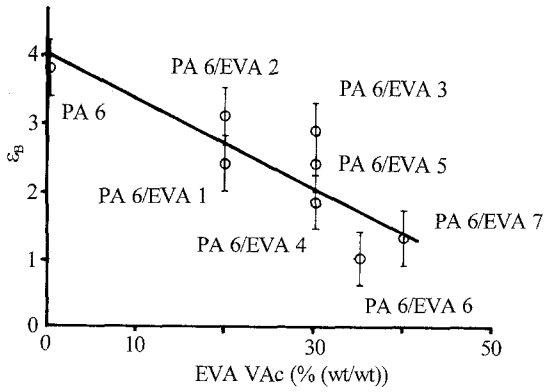

Figure 14 Deformation at break versus VAc content of EVA copolymer for the plain PA6 and PA6/EVA blends.

No relevant effect of the molecular mass of EVA copolymers on ultimate properties of the blended material was found (see Table IX).

4. Conclusion

A study of the influence of molecular structure and composition of EVA copolymers on morphological and structural changes undergone by injection-moulded samples of PA6/EVA blends during uniaxial tensile straining at room temperature up to sample rupture, and on the properties of such blended materials, has been reported.

For the dumb-bell shaped specimens strained to initial cold-drawing it should be noted that the original layered structure is strongly modified by straining. The following three layers are generated:

1. a skin surface where no domains of EVA dispersed phase are observed: the presence of such a layer was already found in previous works [2, 4] and was ascribed to the preferential wetting of the matrix with the mould wall. The thickness of such a layer is, moreover, independent of the straining;

2. an outer layer, S, where the EVA domains are elongated along the draw direction assuming mainly cylindrical shape. The VAc content along the copolymer chain is found to affect the thickness of such a layer and the extent of the deformation undergone therein by EVA domains as follows: the thickness of S increases, for a given copolymer molecular mass, with increasing VAc content along the EVA chain; the extent of the deformation increases, for samples containing copolymers with comparatively lower and intermediate molecular mass, with increasing VAc content, whereas for samples containing copolymers with higher molecular mass, it decreases with increasing VAc content. No systematic dependence of both the thickness of the S layer and the deformation undergone by EVA domains on copolymer molecular mass was, on the other hand, found;

3. a core where the EVA phase segregates in ellipsoidal shaped domains oriented along the draw direction; such a deformation for the blends containing the copolymer with lower and higher molecular mass increases and decreases, respectively, with increasing VAc content along the EVA chain, whereas for the

blends containing copolymers with intermediate molecular mass it is independent of the EVA VAc content. A systematic effect of the EVA molecular mass on its mode and state of dispersion is found only in the blends containing copolymers with lower VAc content along the EVA chain (20% wt/wt). For such samples, in fact, the deformation of EVA domains increases with increasing copolymer molecular mass.

For the dumb-bell-shaped specimens strained to break it is noted that;

4. the T_g value shown by the PA6 fibre is shifted by straining to higher temperature, indicating a reduction of its amorphous molecular mobility;

5. the PA6/EVA fibres show a single T_g, attributed to the PA6 phase, lower than that found for the fibre of plain PA6. Such values, moreover, decrease with increasing VAc along the EVA chain, irrespective of copolymer molecular mass. This finding suggested that by straining, some EVA molecules having a higher number of VAc groups along their chain are able to be dissolved in the amorphous PA6. Such a hypothesis was found to be supported by the noticeable increase of T'_m values shown by the EVA phase in PA6/EVA fibres. Owing to such a dissolution, EVA copolymers with longer PE sequences along their chains were found to remain.

The finding that no T_g attributable to the EVA phase could be detected, was accounted for by supposing that a dissolution of PA6 molecules with low molecular mass into EVA also occurs;

6. The PA6 crystallinity is reduced by straining by about 5%, whereas the crystallinity values shown by PA6 phase in PA6/EVA fibres are higher than that of plain PA6. The former result can be explained by supposing that the conformationally ordered and extended chains of PA6, pulled out by lamellar shearing, lose their lateral order thus becoming amorphous; the latter result may be explained by assuming that, under stress, in the presence of EVA phase, some PA6 chains are able to recrystallize and/or new PA6 ordered phase can be formed during deformation;

7. the mode and state of dispersion of EVA minor component developed in PA6/EVA samples is strongly modified by straining to break. In fact only two layers are found: (i) an outer skin free of EVA domains whose thickness remains unaffected by strain, (ii) a core where the EVA dispersed phase segregates in ellipsoidal-shaped domains indicating that break up and relaxation of the EVA cylindrical-shaped domains, generated in the samples strained to cold-drawing in the S layer, occur.

The number average of the major axis of the ellipsoidal shaped EVA domains, $\bar{D}$, and deformation undergone by such domains, are determined by the VAc content along the EVA chain only in samples containing copolymers with comparatively lower molecular mass. For such samples, in fact, both $\bar{D}$ and the deformation undergone by EVA copolymers increase with increasing VAc content along the EVA chain. Smaller $\bar{D}$ and the lower deformation undergone are shown by the PA6/EVA fibres containing copolymers with intermediate molecular mass, irrespective of the VAc content along the EVA chain. Such a result agrees with that already obtained while studing injection-moulded samples of both the same and different PA6/EVA blends [3, 4].

8. The values of the stress at break, σ_B, shown by PA6/EVA samples are lower than that shown by the plain PA6; moreover, such values were found to be determined by the value of the number average of the major axis, $\bar{D}$, of the ellipsoidal-shaped EVA domains. The trend of σ_B values with $\bar{D}$ of the ellipsoidal-shaped EVA domains shows, in fact, that σ_B increases with increasing copolymer dispersion coarseness. This indicates that the smaller the EVA domains are in size, the higher the stress concentrations induced by external load with subsequent lower overall stress.

In addition, the values of elongation at break, ε_B, shown by PA6/EVA fibres are lower than that of plain PA6, indicating that the presence of EVA domains reduces the capability of the material to be plastically deformed. It should be noted that such values are also found to be determined by the $\bar{D}$ value of the ellipsoidal-shaped EVA domains. The trend of ε_B values with $\bar{D}$ of EVA domains shows, in fact, that ε_B decreases with increasing $\bar{D}$; therefore, the hindrance generated by EVA domains to matrix cold-drawing decreases with increasing dispersion coarseness of the minor component.

The trends of σ_B and ε_B values with the EVA VAc content show, moreover, that σ_B and ε_B values tend to decrease with increasing VAc content, respectively. No relevant effect of the molecular mass of EVA copolymers on ultimate properties of the PA6/EVA blended material was found.

References

1. L. D'ORAZIO, C. MANCARELLA, E. MARTUSCELLI, A. CASALE, A. FILIPPI and F. SPERONI, *J. Mater. Sci.* **21** (1986) 989.
2. *Idem. ibid.* **22** (1987) 429.
3. M. L. ADDONIZIO, L. D'ORAZIO, C. MANCARELLA, E. MARTUSCELLI, A. CASALE and A. FILIPPI, *ibid.* **24** (1989) 2939.
4. M. L. ADDONIZIO, L. D'ORAZIO and E. MARTUSCELLI, *Polymer* **32** (1991) 109.
5. S. CLIMMINO, L. D'ORAZIO, R. GRECO, G. MAGLIO, M. MALINCONICO, C. MANCARELLA, E. MARTUSCELLI, R. PALUMBO and G. RAGOSTA, *Polym. Engng. Sci.*, **24** (1984) 48.
6. M. DOLE and B. WUNDERLICH, *Makromol Chem.* **34** (1959) 29.
7. Z. TADMOR, *J. Appl. Polym. Sci.* **18** (1974) 1753.
8. J. M. SCHULZ, "Polymer Materials Science" (Prentice-Hall, Englewood Cliffs, NJ, 1974).

Received 5 February
and accepted 8 December 1992